

Ultra-relativistic electron beams deflection by quasi-mosaic crystals

Gennady B. Sushko,^{1,*} Andrei V. Korol,^{1,†} and Andrey V. Solov'yov^{1,‡}

¹*MBN Research Center, Altenhöferallee 3, 60438 Frankfurt am Main, Germany*

This paper provides an explanation of the key effects behind the deflection of ultra-relativistic electron beams by means of oriented ‘quasi-mosaic’ Bent Crystals (qmBC). It is demonstrated that accounting for specific geometry of the qmBC and its orientation with respect to a collimated electron beam, its size and emittance is essential for an accurate quantitative description of experimental results on the beam deflection by such crystals. In an exemplary case study a detailed analysis of the recent experiment at the SLAC facility is presented. The methodology developed has enabled to understand the peculiarities in the measured distributions of the deflected electrons. This achievement constitutes an important progress in the efforts towards the practical realization of novel gamma-ray crystal-based light sources and puts new challenges for the theory and experiment in this research area.

PACS numbers: 61.85.+p, 41.60.-m, 41.75.Ht, 02.70.Uu, 07.85.Fv

In recent years [1, 2] significant efforts of the research and technological communities have been devoted to design and practical realization of novel gamma-ray Crystal-based Light Sources (CLS) that can be set up by exposing oriented linear, bent or periodically bent crystals to beams of ultrarelativistic positrons or electrons. Brilliance of radiation emitted in a Crystalline Undulator LS by available positron beams in the photon energy range 10^0 - 10^1 MeV, being inaccessible to conventional synchrotrons, undulators and XFELs, greatly exceeds that of laser-Compton scattering LSs and can be higher than predicted in the Gamma Factory proposal to CERN [3]. The brilliance of CLSs can be further increased by up to 8 orders of magnitude through the process of superradiance by a pre-bunched beam [1]. Manufacturing of CLSs will have significant impact on many research areas in physics, chemistry, biology, material science, technology and medicine, being a subject of the currently running European project ‘N-LIGHT’ [4].

So far oriented crystals exposed to beams of charged particles have been already utilised in a number of applications for beams manipulation, such as steering, bending, extraction and focusing, see [2, 5] and references therein. These and other newly emerging applications in this research area require high quality crystals (bent or periodically bent) and collimated beams of charged ultrarelativistic particles of different energies.

Construction of novel CLSs is a challenging task involving a broad range of correlated research and technological activities [1, 2]. During the last decade a number of papers published in high-impact journals [6–12] on channeling and channeling radiation experiments with bent crystals at different facilities (SLAC, CERN, MAMI). This paper reports on the important progress in this field providing an explanation of the key effects arising by deflection of ultrarelativistic electron and positron beams by means of oriented ‘quasi-mosaic’ Bent Crystals (qmBC). It is demonstrated that account for specific geometry of qmBC and its orientation with respect to a collimated

beam of projectile particles, the beam size and emittance is essential for the quantitative description of the experimental results on the beam deflection by such crystals.

Manufacturing of crystals of different desired geometry is an important technological task in the context of their applications in the gamma-ray CLSs and the aforementioned experiments. The systematic review of different technologies exploited for manufacturing of crystals of different type, geometry, size, quality, etc is given in [1, 2, 5]. A short summary of several relevant approaches that have been utilized to produce bent crystals is provided in Supplemental Material (SM).

The high-quality qmBCs structures with desirable and fully controllable parameters have been manufactured for the aforementioned channeling experiments by the following means [13–15]. When a moment of force is applied to a crystalline material, some secondary curvatures may arise within the solid [16]. A well known secondary deformation is the anticlastic curvature that occurs in a medium subjected to two moments. In particular, it occurs in the perpendicular direction with respect to the primary curvature. When the two curvatures are combined, the deformed crystal acquires the shape of a saddle. In contrast to an amorphous medium physical properties of crystals may be strongly anisotropic. A secondary deformation caused by anisotropic effects is the ‘quasi-mosaic’ (QM) curvature [17]. QM bent crystals belong to a class of bent crystals featuring two curvatures of two orthogonal crystallographic planes. As a crystal is bent to a primary curvature by external forces, a secondary curvature can be generated within the crystal, i.e. the QM curvature [18]. This curvature is always absent in an isotropic material. The planes bent by the QM effect are orthogonal to the main surface of the plate.

In order to understand the effects arising during channeling of charged particles through qmBC one should consider the geometry of such a crystal and its orientation with respect to a beam of projectile particles. This geometry is shown in Fig. 1. For the sake of clarity the

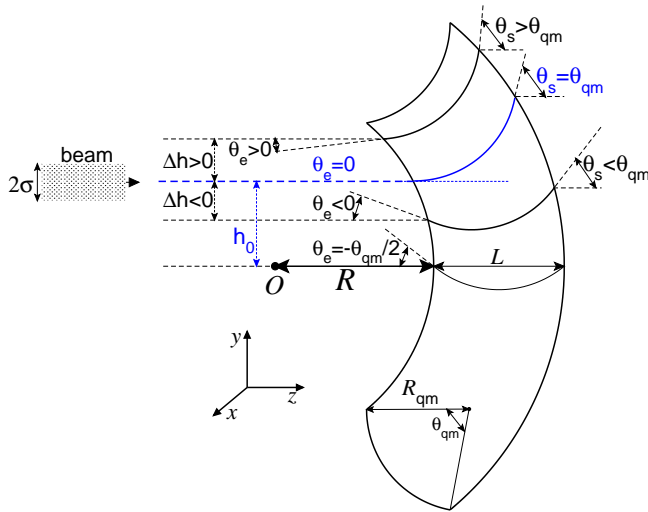


FIG. 1. Geometry of the QM bending of a crystal plate of thickness L and its orientation with respect to a beam of projectile particles (shaded rectangle). See explanations in the text.

case of planar channeling is addressed below.

Consider a crystal whose planes, which are parallel to the (xy) plane, are bent with primary curvature of radius R . The center O of the curvature lies on the z axis, which runs through the crystal center. The primary deformation causes the QM bending of the planes. Let us assume that both R and the QM bending radius R_{qm} greatly exceed the crystal thickness L and that the anticlassic curvature is much smaller than $1/R$. These conditions have been met for the qmBC samples used in the experiments [6–12]. The QM bending angle is defined as follows

$$\theta_{\text{qm}} = \frac{L}{R_{\text{qm}}} \ll 1. \quad (1)$$

To start with, let us assume an ideally collimated narrow beam (i.e. that of zero divergence and zero beam size in the y direction, $\sigma_\phi, \sigma \rightarrow 0$) incident on the crystal along the z direction. In the case of planar channeling the beam size and divergence in the x direction play no role and thus are not considered below.

At the crystal entrance, the angle θ_e between the beam direction and a tangent line to the QM bent plane depends on the beam displacement h along the y -axis:

$$\theta_e(h) = \frac{h}{R} - \frac{\theta_{\text{qm}}}{2} = \frac{\Delta h}{R} \quad (2)$$

where $\Delta h = h - h_0$ and h_0 denotes the displacement for which the entrance angle $\theta_e = 0$, i.e. the tangent line is parallel to the z axis:

$$h_0 = \frac{\theta_{\text{qm}} R}{2}. \quad (3)$$

A probability of a particle to be accepted into the channeling mode becomes significant if θ_e does not exceed

Lindhard's critical angle θ_L . Then, using (2) one finds the maximum value of Δh

$$\Delta h_{\text{max}} = \theta_L R, \quad (4)$$

so that the channeling condition is met for the particles entering the crystal with the vertical displacement h within the interval $h_0 - \Delta h_{\text{max}} \leq h \leq h_0 + \Delta h_{\text{max}}$.

At the crystal exit, the angle θ_s between the tangent line to the plane and the beam direction is also unambiguously related to the vertical displacement via

$$\theta_s(h) = \theta_e(h) + \theta_{\text{qm}}. \quad (5)$$

Hence, the projectiles that are accepted at $y = h$ and channel through the whole crystal are deflected by the angle lying within the interval $\theta_s(h) \pm \theta_L$.

The particles that enter the crystal with $\Delta h < 0$ can experience either volume capture [19] or volume reflection [20] in the course of propagation through the crystal. The geometry analysis for these regimes is given in SM.

The particles that enter with $\Delta h > \theta_L R$ are neither captured to the channeling mode nor experience the volume reflection. Such particles experience multiple scattering which becomes more and more similar to multiple scattering as in amorphous medium with increase of Δh .

Now let us consider a Gaussian beam centered at $y = h$ having finite width σ and divergence σ_ϕ in the y direction. These quantities as well as their product $\varepsilon = \sigma\sigma_\phi$, called the beam emittance, are the characteristics commonly used in the accelerator physics. As demonstrated below it is important for them by interpreting the aforementioned experiments on the beam propagation through oriented qmBC crystals which have been carried out with beams having different emittance. Thus, at SLAC the narrow beams with $\sigma \leq 10 \mu\text{m}$ and $\gamma\varepsilon \lesssim 1 \text{ m}\cdot\mu\text{rad}$ have been used [21] (γ stands for the Lorentz relativistic factor). Contrary, the wider beams $\sigma \sim 10^2 \mu\text{m}$ have been exploited at the MAMI facility [22].

Due to the finite values of the beam size σ and divergence σ_ϕ different particles of the beam enter the crystal having different initial values of h and θ_e .

In what follows the discussion is focused on the analysis of the experiment at SLAC [7], although the physics discussed and the conclusions drawn are largely applicable to other aforementioned experiments with oriented qmBC. At the SLAC experiment a $60 \mu\text{m}$ thick silicon (111) qmBC was exposed to a 6.3 GeV electron beam. The curvature radii quoted are $R_{\text{qm}} = 15 \text{ cm}$ and $R = 4.4 \text{ cm}$. Using these values in (1) and (3) one finds $\theta_{\text{qm}} = 400 \mu\text{rad}$ and $h_0 = 8.80 \mu\text{m}$. For a 6.3 GeV electron Lindhard's critical angle is $80 \mu\text{rad}$ [7]. This value results in $\Delta h_{\text{max}} = 3.52 \mu\text{m}$ for the maximum displacement consistent with the channeling condition, see Eq. (4).

Numerical modeling of the channeling and related phenomena beyond the continuous potential framework can be carried out by means of the multi-purpose software

package MBN EXPLORER [23–25] and a supplementary special multitask software toolkit MBN STUDIO [26]. The MBN EXPLORER was originally developed as a universal computer program to allow multiscale simulations of structure and dynamics of molecular systems.

MBN EXPLORER simulates the motion of relativistic projectiles along with dynamical simulations of the environment, crystalline structures included crystalline structures [24]. The computation accounts for the interaction of projectiles with separate atoms of the environment, whereas a variety of interatomic potentials implemented supports rigorous simulations of various media. Overview of the results on channeling and radiation of charged particles in oriented linear, bent and periodically bent crystals simulated by means of MBN EXPLORER and MBN STUDIO can be found in [1, 2, 5, 25].

To model propagation of particles through qmBCs by means of MBN EXPLORER and MBN STUDIO further development of the algorithm for the atomistic simulations of the crystalline media has been performed in this work. The implemented algorithm enabled simulations of a qmBC defined through the transformation of the unperturbed crystalline medium by the two curvature radii R and R_{qm} , positioning of a qmBC with respect to the beam direction and the relativistic molecular dynamics in such environment. The results reported below have been obtained by means of this newly implemented algorithm.

Now let us analyze the results of simulations and compare them with experimental data. As a first step, consider a narrow particle beam as a probe for different particle propagation regimes in oriented qmBCs discussed above. Figure 2 shows simulated distributions for the beam with $\sigma = 0.1 \mu\text{m}$ and $\sigma_\phi = 30 \mu\text{rad}$. In this figure as well as in all the follow up ones, the experimental data from [7] are also shown. The figure illustrates the change in the angular distribution profile due to variation of the displacement h at the entrance. The change in the angular distribution due to variation of the beam divergence at the fixed value of h is illustrated by Fig. S1 in SM.

All the simulated and the measured angular distributions have the characteristic pattern of the two well pronounced peaks interlinked by an intermediate region. The left peak in the vicinity of the zero deflection angle describes a fraction of particles propagating through the qmBC in the forward direction. This group of particles experience multiple scattering resulting in the broadening of the initial distribution of beam particles. Small shift of the peak to the region of negative angles is due to the volume reflection of the particles from the bent crystalline planes. As discussed in SM this effect becomes more pronounced at the entrance points within the region $-h_0 < h < h_0$. The right peak is formed by the particles accepted to the channeling regime at the entrance and deflected to the angle $\theta_s(h)$ according to Eq. (5). The position of the channeling peak is determined by the value h corresponding to the beam center at the

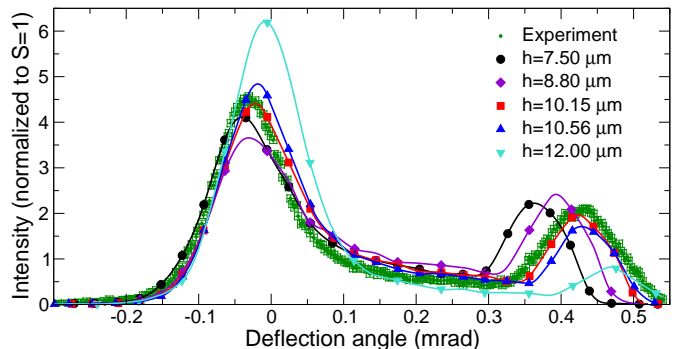


FIG. 2. Simulated distributions (solid lines with symbols) of the deflected narrow beam ($\sigma = 0.1 \mu\text{m}$) obtained for fixed beam divergence $\sigma_\phi = 30 \mu\text{rad}$ but different values of the displacement h . Symbols with error bars in this and all the follow up figures correspond to the experimental distribution [7] with the background subtracted. All dependences are normalized to unit area.

entrance point and the width of the peak is determined by the distribution of $\theta_c(h)$ for the particles of the beam and by Lindhard’s angle. The channeling peak is also influenced by the dechanneling process that is responsible for the formation of the distribution of the deflected particles in the region between the two peaks.

The curve corresponding to $h = 8.8 \mu\text{m}$ represents the reference case $h = h_0$. At $h = 7.5 \mu\text{m}$, i.e. when $h < h_0$, the volume reflection becomes stronger than in the reference case resulting in the shift of the main maximum towards negative deflection angles. The channeling peak is also left shifted in accordance with Eq. (5). At $h = 10.15 \mu\text{m}$ the angular distribution becomes very close to the experimentally observed one in the whole range of angles. As h increases further the correspondence with the experimental data worsens. Already at $h = 10.56 \mu\text{m}$ one can see the visible shift of the both maxima to the right as well as the change in their heights. At $h = 12.0 \mu\text{m}$, which is close to the maximum displacement consistent with the channeling condition, the channeling peak becomes strongly suppressed and shifted further to the right. At the same time, the main peak becomes more powerful and centered around $\theta_s = 0$, which indicates the increase in the number of particles moving in the forward direction and experiencing multiple scattering.

Figure 2 shows that at $h = 10.15 \mu\text{m}$ a nearly ideal agreement with the experimental data can be achieved for the beam divergence $\sigma_\phi = 30 \mu\text{rad}$. Further increase of σ_ϕ results in decreasing the channeling fraction and enhancing the volume reflection, see Fig. S1 in SM.

In spite of the very good agreement obtained for the narrow beam one needs to note that in experiments the beam sizes are much larger than $0.1 \mu\text{m}$. Thus, the parameters of the electron beam at SLAC are $\sigma = 7 \mu\text{m}$, $\sigma_\phi \sim 10 \mu\text{rad}$, $\gamma\varepsilon \approx 1 \text{ m-}\mu\text{rad}$ [21]. Therefore, additional analysis of the angular distributions of deflected particles

for wider beams is needed.

In the case of a wide beam centered at h most of the beam particles enter the crystal having the y coordinates within the interval from $h - \sigma$ to $h + \sigma$ and the corresponding entrance angles θ_e . Therefore, the distribution of deflected particles becomes a superposition of different propagation scenarios discussed in the context of the qmBC geometry shown in Fig. 2. Such situation is illustrated by Fig. 3 (left) for a wide beam with the emittance $\gamma\varepsilon \approx 0.4$ m- μ rad. One observes a significant discrepancy between the simulated distribution and the experimental curve. It is seen that at $h > h_0$ the simulated fraction of channeling particles is underestimated while the dechanneling is overestimated. Consequently, the fraction of non-accepted particles experiencing multiple scattering in the forward direction becomes larger than in the experiment. The discrepancy increases with the beam emittance (see Fig. S2 in SM for $\gamma\varepsilon \approx 1$ m- μ rad). At $h < h_0$ the more pronounced becomes the manifestation of the volume reflection and volume capture effects.

The discrepancy can be attributed to some subtraction procedure adopted to process the experimental data [7]. Basing on the description sketched in the cited paper one can deduce that the experimental dependence shown has been obtained by subtracting part of the distribution (approximately one third) measured for a non-oriented crystal corresponding to the amorphous silicon.

In accordance with this the following procedure to modify the simulated spectra has been adopted: (i) the angular distribution $dN_{\text{am}}/d\theta$ has been simulated for a 60 μm thick amorphous silicon; (ii) some fraction x of $dN_{\text{am}}/d\theta$ has been subtracted from the distribution $dN_{\text{qm}}/d\theta$ obtained for the QM crystal.

Figures 3 (right) and 4 show the results of simulations obtained by means of the subtraction procedure described above. Different values of x indicated in Fig. 4 correspond to different fractions of subtracted particles as it is explicitly indicated in Fig. 3 (right). This figure demonstrates that the subtraction procedure enables to restore the nearly perfect agreement between the simulated and the experimental distributions for wider beams, see red curves. With the further increase in the emittance the agreement of the simulation results and experiment worsens, although still remains fairly reasonable at $\gamma\varepsilon = 1$ m- μ rad (see Fig. S3 in SM). Even in this case, the agreement of the simulation results with experiment is visibly better as compared to what is presented in [7].

The quantitative analysis of the angular distribution of ultrarelativistic electrons deflected by oriented qmBCs presented in our paper demonstrates the good agreement with experimental data reported in [7]. It was achieved by accounting for (i) the specific geometry of such crystals and their orientation with respect to the projectile beam and (ii) the realistic beam characteristics (size, divergence and emittance). Remaining discrepancies can be attributed to the unknown concrete values of the beam

characteristics, details of the experimental setup as well as to the lack of information on the subtraction procedure adopted in [7] for the quantitative characterization of the measured distributions. It is highly desirable that such information is provided when presenting the experimental data since it allows for its independent unambiguous theoretical and computational validation. Important issue concerns also accurate measurement and computational analysis of the characteristics of radiation that accompany passage of ultra-relativistic projectiles through oriented crystals. Such knowledge is essential for better planning of accelerator-based experiments and for full interpretation of their results thus enabling progress towards optimal design and practical realization of the novel gamma-ray CLSs.

The work was supported in part by the DFG Grant (Project No. 413220201) and by the H2020 RISE-NLIGHT project (GA 872196). We acknowledge the Frankfurt Center for Scientific Computing (CSC) for providing computer facilities.

* sushko@mbnexplorer.com

† korol@mbnexplorer.com; On leave from: St. Petersburg State Marine Technical University, Leninsky ave. 101, 198262 St. Petersburg, Russia

‡ solovyov@mbnresearch.com; On leave from: Ioffe Physical-Technical Institute, Politekhnicheskaya 26, 194021 St. Petersburg, Russia

- [1] A. V. Korol and A. V. Solov'yov, *Crystal-based intensive gamma-ray light sources*. *Europ. Phys. J. D* **74**, 201 (2020).
- [2] A. V. Korol and A. V. Solov'yov, *All-atom relativistic molecular dynamics simulations of channeling and radiation processes in oriented crystals*. *Europ. Phys. J. D* **75**, 207 (2021).
- [3] M. Krasny, The Gamma Factory proposal for CERN. *CERN Proc.* **1**, 249 (2018).
- [4] <http://www.mbnresearch.com/N-Light/main>
- [5] A. V. Korol, A. V. Solov'yov, and W. Greiner, *Channeling and Radiation in Periodically Bent Crystals*, Second ed., Springer-Verlag, Berlin, Heidelberg, 2014.
- [6] A. Mazzolari, E. Bagli, L. Bandiera, V. Guidi, H. Backe, W. Lauth, V. Tikhomirov, A. Berra, D. Lietti, M. Prest, E. Vallazza, and D. De Salvador, *Steering of a sub-GeV electron beam through planar channeling enhanced by rechanneling*. *Phys. Rev. Lett.* **112**, 135503 (2014).
- [7] U. Wienands, T. W. Markiewicz, J. Nelson, R. J. Noble, J. L. Turner, U. I. Uggerhøj, T. N. Wistisen, E. Bagli, L. Bandiera, G. Germogli, V. Guidi, A. Mazzolari, R. Holtzapfel, and M. Miller, *Observation of deflection of a beam of multi-GeV electrons by a thin crystal*. *Phys. Rev. Lett.* **114**, 074801 (2015).
- [8] L. Bandiera, E. Bagli, G. Germogli, V. Guidi, A. Mazzolari, H. Backe, W. Lauth, A. Berra, D. Lietti, M. Prest, D. De Salvador, E. Vallazza, and V. Tikhomirov, *Investigation of the electromagnetic radiation emitted by sub-GeV electrons in a bent crystal*. *Phys. Rev. Lett.* **115**, 025504 (2015).

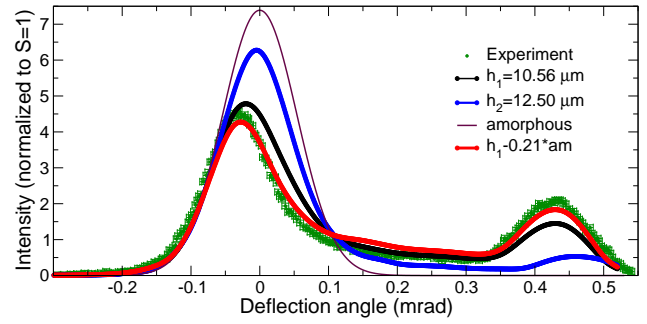
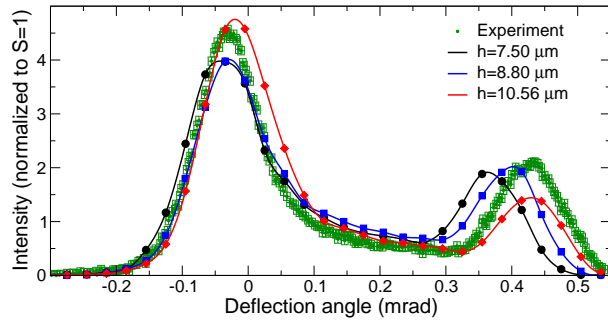


FIG. 3. Simulated distributions for $\sigma = 1 \mu\text{m}$ and $\sigma_\phi = 30.4 \mu\text{rad}$. *Left panel.* Distributions without subtraction obtained for different h values. *Right panel.* Distributions for $h_1 = 10.56 \mu\text{m}$ modified by subtracting the fraction $x = 0.21$ of deflected particles propagating in amorphous silicon ('am').

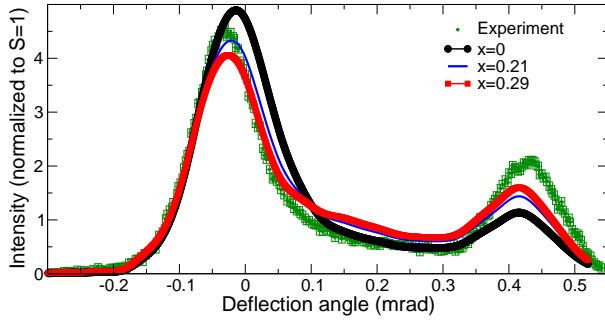


FIG. 4. Simulated distributions for beam size $\sigma = 2 \mu\text{m}$ and divergence $\sigma_\phi = 30.4 \mu\text{rad}$ ($\gamma\varepsilon = 0.75 \text{ m-}\mu\text{rad}$), and initial coordinate $h = 10.56 \mu\text{m}$ obtained without ($x = 0$) and with subtraction of the fraction x (as indicated) of the amorphous background.

[9] L. Bandiera, E. Bagli, V. Guidi, A. Mazzolari, A. Berra, D. Lietti, M. Prest, E. Vallazza D. De Salvador, and V. Tikhomirov. *Broad and Intense Radiation Accompanying Multiple Volume Reflection of Ultrarelativistic Electrons in a Bent Crystal*. Phys. Rev. Lett. **111**, 255502 (2013).

[10] A. Mazzolari, M. Romagnoni, R. Camattari, E. Bagli, L. Bandiera, G. Germogli, V. Guidi, and G. Cavoto. *Bent crystals for efficient beam steering of multi TeV-particle beams*. Eur. Phys. J. C **78**, 720 (2018).

[11] A.I. Sytov, V. Guidi, V. V. Tikhomirov, E. Bagli, L. Bandiera, G. Germogli, and A. Mazzolari. *Planar channeling and quasicchanneling oscillations in a bent crystal*. Eur. Phys. J. C **76**, 77 (2016).

[12] T. N. Wistisen, U. I. Uggerhøj, U. Wienands, T. W. Markiewicz, R. J. Noble, B. C. Benson, T. Smith, E. Bagli, L. Bandiera, G. Germogli, V. Guidi, A. Mazzolari, R. Holtzapple, and S. Tucker. *Channeling, volume reflection, and volume capture study of electrons in a bent silicon crystal*. Phys. Rev. Acc. Beams **19**, 071001 (2016).

[13] V. Guidi, A. Mazzolari, D. De Salvador, and A. Carnera. *Silicon crystal for channelling of negatively charged particles*. J. Phys. D: Appl. Phys. **42**, 182005 (2009).

[14] R. Camattari, V. Guidi, V. Bellucci, and A. Mazzolari. *The quasi-mosaic effect in crystals and its application in*

modern physics. J. Appl. Cryst. **48**, 977 (2015).

[15] A. Mazzolari, M. Romagnoni, R. Camattari, E. Bagli, L. Bandiera, G. Germogli, V. Guidi, G. Cavoto. R. Camattari, V. Guidi, V. Bellucci, and A. Mazzolari. *Bent crystals for efficient beam steering of multi TeV-particle beams*. Eur. Phys. J. C **78**, 720 (2018).

[16] S. Lekhnitskii. *Theory of Elasticity of an Anisotropic Body*. Moscow: Mir Publishers, 1981.

[17] O. I. Sumbaev. *Reflection of Gamma-Rays From Bent Quartz Plates*. JETP **5**, 1042 (1957).

[18] Y. Ivanov, A. Petrunin, and V. Skorobogatov. *Observation of the elastic quasi-mosaicity effect in bent silicon single crystals*. JETP Lett. **81**, 977 (2005).

[19] A. M. Taratin and S. A. Vorobiev. *Volume trapping of protons in the channeling regime in a bent crystal*. Phys. Lett. **115**, 398 (1986).

[20] A. M. Taratin and S. A. Vorobiev. *Volume reflection of high-energy charged particles in quasi-channeling states in bent crystals*. Phys. Lett. **119**, 425 (1987).

[21] Mauro Pivi and Carsten Hast. *ESTB End Station Test Beam Design, Performance, Infrastructure, Status*. ESTB 2012 Users Meeting, SLAC (August 23, 2012).

[22] H. Backe, P. Kunz, W. Lauth, and A. Rueda. *Planar Channeling Experiments with Electrons at the 855-MeV Mainz Microtron*. Nucl. Instrum. Methods B **266**, 3835 (2008).

[23] I. A. Solov'yov, A. V. Yakubovich, P. V. Nikolaev, I. Volkovets, and A. V. Solov'yov. *MesoBioNano Explorer – A universal program for multiscale computer simulations of complex molecular structure and dynamics..* J. Comp. Phys. **33**, 2412 (2012).

[24] G. B. Sushko, V. G. Bezchastnov, I. A. Solov'yov, A. V. Korol, W. Greiner, and A. V. Solov'yov. *Simulation of ultra-relativistic electrons and positrons channeling in crystals with MBN Explorer*. J. Comp. Phys. **252**, 404 (2013).

[25] I. A. Solov'yov, A. V. Korol, and A. V. Solov'yov. *Multiscale Modeling of Complex Molecular Structure and Dynamics with MBN Explorer*. Springer International Publishing, Cham, Switzerland (2017).

[26] G. B. Sushko, I. A. Solov'yov, and A. V. Solov'yov. *Modeling MesoBioNano systems with MBN Studio made easy*. J. Mol. Graph. Model. **88**, 247 (2019).

Supplemental Material for "Ultra-relativistic electron beams deflection by quasi-mosaic crystals"

Gennady B. Sushko,^{1,*} Andrei V. Korol,^{1,†} and Andrey V. Solov'yov^{1,‡}

¹*MBN Research Center, Altenhöferallee 3,
60438 Frankfurt am Main, Germany*

Abstract

In what follows some explanatory material, additional to the main text, is presented.

METHODS FOR MANUFACTURING OF BENT CRYSTALS

Approaches that have been utilised to produce bent crystals include mechanical scratching [1], laser ablation technique [2], grooving method [3, 4], tensile/compressive strips deposition [3, 5, 6], ion implantation [7]. The most recent techniques proposed are based on sandblasting one of the major sides of a crystal to produce an amorphized layer capable of keeping the sample bent [8] and on pulsed laser melting processing that produces localized and high-quality stressing alloys on the crystal surface [9].

To increase the bending curvature one can rely on production of graded composition strained layers in an epitaxially grown $\text{Si}_{1-x}\text{Ge}_x$ superlattice [10, 11]. Both silicon and germanium crystals have the diamond structure with close lattice constants. Replacement of a fraction of Si atoms with Ge atoms leads to bending crystalline directions. By means of this method sets of periodically bent crystals have been produced and used in channeling experiments [12]. A similar effect can be achieved by graded doping during synthesis to produce diamond superlattice [13]. Both boron and nitrogen are soluble in diamond, however, higher concentrations of boron can be achieved before extended defects appear [13, 14]. The advantage of a diamond crystal is radiation hardness allowing it to maintain the lattice integrity in the environment of very intensive beams [15].

GEOMETRY ANALYSIS FOR THE VOLUME CAPTURE AND REFLECTION REGIMES

Particles entering the crystal in the region $\Delta h < 0$ can experience either the volume capture [16] or the volume reflection [17] of the curved crystalline planes during their propagation through the crystal volume. These events take place at the points in space at which the particles trajectories become tangent to the crystalline planes. This condition is fulfilled for most of the particle trajectories entering the crystal at distances $-h_0 < h < h_0$. with respect to the central line corresponding to $h = 0$. For a given h the point of the volume capture and the volume reflection is positioned at the distance $L/2 - R_{\text{qm}}h/R$ from the particle entrance point to the crystal. Thus this distance is equal to zero at $h = h_0$ and to L at $h = -h_0$. Particles moving in the channeling regime after the volume capture exit the

crystal at

$$\theta_s^{vc}(h) = \theta_e(h) + \frac{\theta_{qm}}{2} + \frac{h}{R} \quad (S1)$$

In the process of volume reflection particles are deflected on the characteristic angle θ_{vr} which does not depend on the choice of h and the location of the volume reflection event in space. The angle θ_{vr} is determined by the radius R_{qm} and the particle energy. After the volume reflection particles experience multiple scattering within the remaining crystal volume and exit the crystal at the characteristic angle

$$\theta_s^{vr}(h) = \theta_{vr} \quad (S2)$$

ADDITIONAL SIMULATED ANGULAR DISTRIBUTIONS

Figure S1 illustrates the change in the angular distribution profile due to variation of the beam divergence σ_ϕ . The coordinate h at the entrance is fixed at the value $h = 10.15 \mu\text{m}$. It is seen that a nearly ideal agreement with the experimental data is achieved for $\sigma_\phi = 30 \mu\text{rad}$. Further increase in the divergence results in decreasing the fraction of channeled particles and enhancing the volume reflection, lowering and shift to the left of the main peak and growth of its left shoulder.

The distributions of deflected particles for a wide beam ($\sigma = 7 \mu\text{m}$) with normalized emittance $1 \text{ m-}\mu\text{rad}$ calculated for different values of the coordinate h are presented in Fig. S2. It becomes a superposition of different propagation scenarios discussed. A significant discrepancy of the simulated distributions with respect to the experimental curve can be observed. In particular, for $h > h_0$ the simulated fraction of channeling particles is underestimated, while dechanneling is overestimated. Consequently, the simulated fraction of non-accepted particles experiencing multiple scattering in the forward direction becomes larger than it is on the experimental curve. At $h < h_0$ the more pronounced becomes the manifestation of the volume reflection and the volume capture effects.

Figure S3 shows the results of simulations obtained by means of the subtraction procedure described in the main text. Different values of x correspond to different fractions of the distribution in the amorphous silicon subtracted from the distributions simulated for the qmBC. Compared to Fig. 4 in the main text, this figure illustrates that further increase in

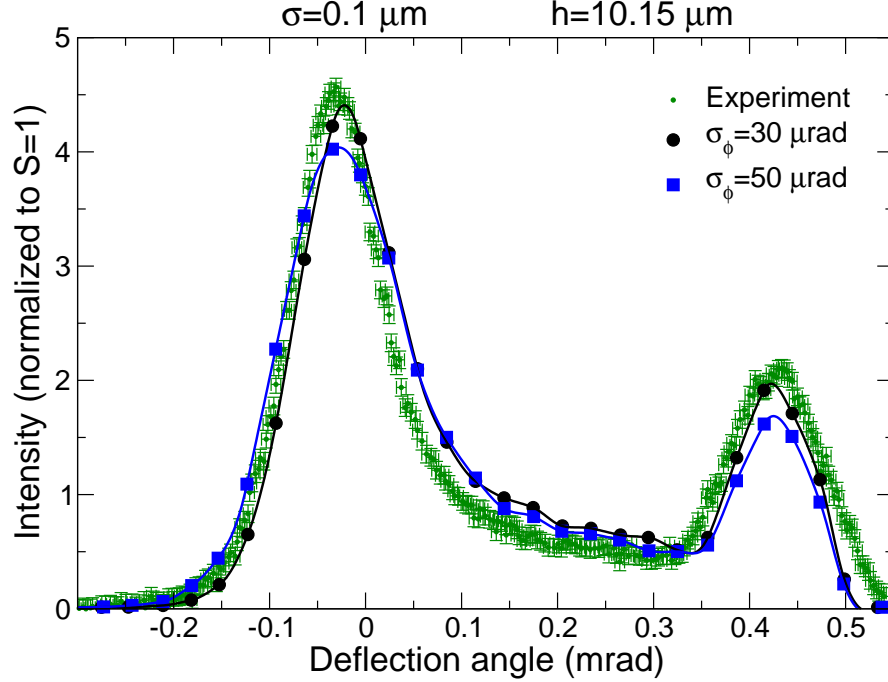


FIG. S1. Simulated distributions (solid lines with symbols) of the deflected narrow beam ($\sigma = 0.1 \mu\text{m}$) obtained for the fixed value $h = 10.15 \mu\text{m}$ of the displacement from the central line (see Figure 1 in the Main Text) and two values of the beam divergences σ_ϕ as indicated. Symbols with error bars correspond to the experimental distribution [18] with the background subtracted. All dependences are normalized to unit area.

the emittance does not improve agreement between the simulation results and the experiment [18].

* sushko@mbnexplorer.com

† korol@mbnexplorer.com; On leave from: St. Petersburg State Marine Technical University, Leninsky ave. 101, 198262 St. Petersburg, Russia

‡ solovyov@mbnresearch.com; On leave from: Ioffe Physical-Technical Institute, Politekhnikheskaya 26, 194021 St. Petersburg, Russia

[1] S. Bellucci, S. Bini, V. M. Biryukov, Yu. A. Chesnokov, et al. *Experimental study for the feasibility of a crystalline undulator*. Phys. Rev. Lett. **90**, 034801 (2003).

[2] P. Balling, J. Esberg, K. Kirsebom, D. Q. S. Le, U. I. Uggerhøj, S. H. Connell, J. Härtwig,

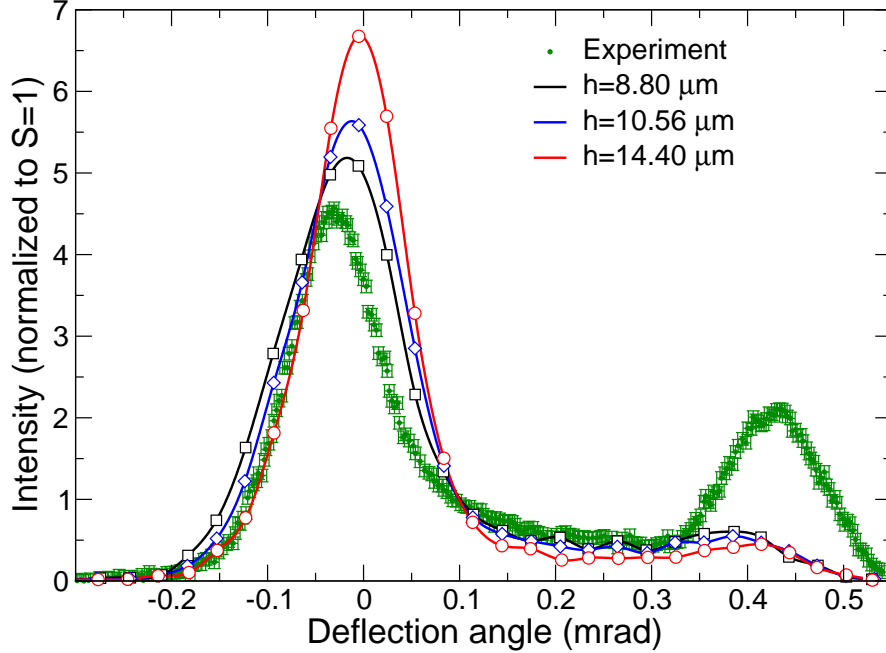


FIG. S2. Simulated distributions for $\sigma = 7 \mu\text{m}$ and $\sigma_\phi = 11.6 \mu\text{rad}$ (normalized emittance $\gamma\varepsilon = 1 \text{ m-}\mu\text{rad}$). Symbols with error bars correspond to the experimental distribution [18] with the background subtracted. All dependences are normalized to unit area.

- F. Masiello, and A. Rommeveaux. *Bending diamonds by femto-second laser ablation*. Nucl. Instrum. Meth. B **267**, 2952 (2009).
- [3] V. Guidi, A. Antonioni, S. Baricordi, F. Logallo, C. Malagù, E. Milan, A. Ronzoni, M. Stefancich, G. Martinelli, and A. Vomiero. *Tailoring of silicon crystals for relativistic-particle channeling*. Nucl. Instrum. Meth. B **234**, 40 (2005).
- [4] E. Bagli, L. Bandiera, V. Bellucci, A. Berra, R. Camattari, D. De Salvador, G. Germogli, V. Guidi, L. Lanzoni, D. Lietti, A. Mazzolari, M. Prest, V. V. Tikhomirov, and E. Valla. *Experimental evidence of planar channeling in a periodically bent crystal*. Eur. Phys. J. C **74**, 3114 (2014).
- [5] V. Guidi, A. Mazzolari, G. Martinelli, and A. Tralli. *Design of a crystalline undulator based on patterning by tensile Si_3N_4 strips on a Si crystal*. Appl. Phys. Lett. **90**, 114107 (2007).
- [6] V. Guidi, L. Lanzoni, and A. Mazzolari. *Patterning and modeling of mechanically bent silicon plates deformed through coactive stresses*. Thin Solid Films **520**, 1074 (2011).
- [7] V. Bellucci, R. Camattari, V. Guidi, A. Mazzolari, G. Paterno, G. Mattei, C., Scian, and L. Lanzoni. *Ion implantation for manufacturing bent and periodically bent crystals*. Appl. Phys.

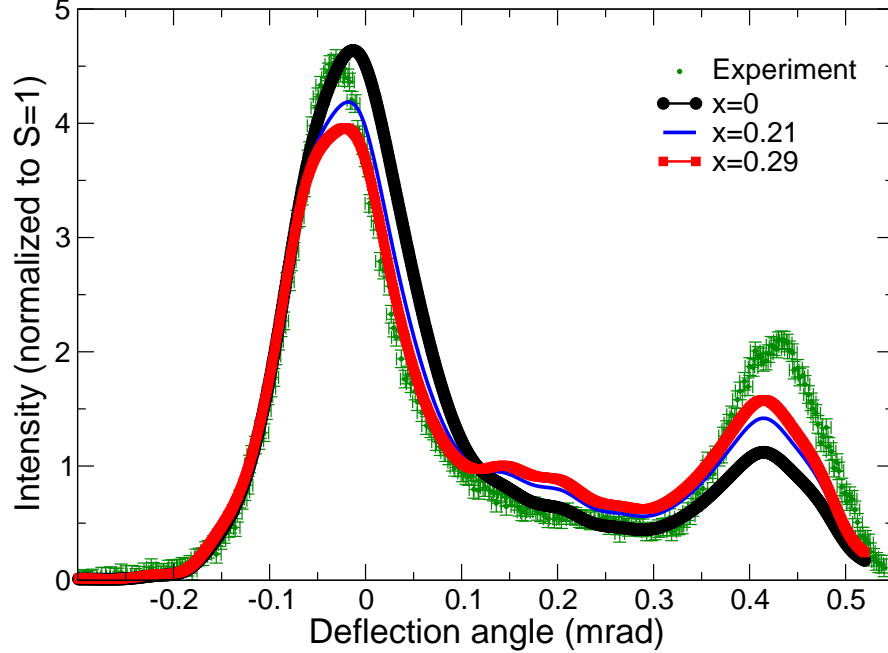


FIG. S3. Simulated distributions for beam size $\sigma = 2 \mu\text{m}$ and divergence $\sigma_\phi = 40.6 \mu\text{rad}$ (normalized emittance $\gamma\varepsilon = 1 \text{ m-}\mu\text{rad}$), and initial coordinate $h = 10.56 \mu\text{m}$ obtained without ($x = 0$) and with subtraction of the fraction x (as indicated) of the amorphous background. All dependences are normalized to unit area.

Lett. **107**, 064102 (2015).

- [8] R. Camattari, G. Paternò, M. Romagnoni, V. Bellucci, A. Mazzolari and V. Guidi. *Homogeneous self-standing curved monocrystals, obtained using sandblasting, to be used as manipulators of hard X-rays and charged particle beams*. J. Appl. Cryst. **50** (2017) 145-151.
- [9] F. Cristiano, M. Shayesteh, R. Duffy, K. Huet, F. Mazzamuto, Y. Qiu, M. Quillec, H. H. Henrichsen, P. F. Nielsen, D. H. Petersen, A. La Magna, G. Caruso, and S. Boninelli. *Defect evolution and dopant activation in laser annealed Si and Ge*. Mat. Scie. in Semicond. Process. **42** (2016) 188-195
- [10] S. A. Bogacz and J. B. Ketterson. *Possibility of obtaining coherent radiation from a solid state undulator*. J. Appl. Phys. **60**, 177 (1986).
- [11] U. Mikkelsen and E. Uggerhøj. *A crystalline undulator based on graded composition strained layers in a superlattice*. Nucl. Instrum. Meth. B **160**, 435 (2000).
- [12] H. Backe, D. Krambrich, W. Lauth, K. K. Andersen, J. L. Hansen, and U. I. Uggerhøj. *Radiation emission at channeling of electrons in a strained layer $\text{Si}_{1-x}\text{Ge}_x$ undulator crystal*.

- Nucl. Instrum. Meth. B **309**, 37 (2013).
- [13] T. N. Tran Thi, J. Morse, D. Caliste, B. Fernandez, D. Eon, J. Härtwig, C. Barbay, C. Mer-Calfati, N. Tranchant, J. C. Arnault, T. A. Lafford, and J. Baruchel. *Synchrotron Bragg diffraction imaging characterization of synthetic diamond crystals for optical and electronic power device applications*. J. Appl. Cryst. **50**, 561 (2017).
- [14] B. G. de la Mata, A. Sanz-Hervás, M. G. Dowsett, M. Schwitters, and D. Twitchen. *Calibration of boron concentration in CVD single crystal diamond combining ultralow energy secondary ions mass spectrometry and high resolution X-ray diffraction*. Diamond and Rel. Mat. **16**, 809 (2007).
- [15] U. Uggerhøj. *The interaction of relativistic particles with strong crystalline fields*. Rev. Mod. Phys. **77**, 1131 (2005).
- [16] A. M. Taratin and S. A. Vorobiev. *"Volume trapping" of protons in the channeling regime in a bent crystal*. Phys. Lett. **115**, 398 (1986).
- [17] A. M. Taratin and S. A. Vorobiev. *Volume reflection of high-energy charged particles in quasi-channeling states in bent crystals*. Phys. Lett. **119**, 425 (1987).
- [18] U. Wienands, T. W. Markiewicz, J. Nelson, R. J. Noble, J. L. Turner, U. I. Uggerhøj, T. N. Wistisen, E. Bagli, L. Bandiera, G. Germogli, V. Guidi, A. Mazzolari, R. Holtzapple, and M. Miller. *Observation of deflection of a beam of multi-GeV electrons by a thin crystal*. Phys. Rev. Lett. **114**, 074801 (2015).